

Scanning Electrochemical Microscopy of Living Cells. 4. Mechanistic Study of Charge Transfer Reactions in Human Breast Cells

Biao Liu, Susan A. Rotenberg, and Michael V. Mirkin*

Department of Chemistry and Biochemistry, Queens College–CUNY, Flushing, New York 11367

Scanning electrochemical microscopy (SECM) has recently been employed for probing the redox properties of individual mammalian cells. It was shown that intracellular redox activity can be probed noninvasively by measuring the rate of mediator regeneration by the cell. Depending on the properties of the mediator species (e.g., formal potential, ionic charge, and hydrophobicity), different steps can limit the rate of the mediator regeneration reaction. This paper describes the evaluation of several factors that determine the rates of different steps of the process. These include intracellular concentration of redox centers, mixed redox potential inside the cell, and the rate of membrane permeation by mediator species. The kinetic analysis has been carried out to clarify the origins of different rates of the overall charge-transfer reaction in different cell types and with different redox mediators. The results can be used to facilitate differentiation between different types of cells, for example, normal and metastatic breast cells, on the basis of differences in redox responses.

The introduction of a wide range of spectroscopic^{1–3} and electrochemical^{4,5} methods and separation techniques⁶ made possible the investigation of biologically important reactions at single cell and subcellular levels. These include a number of intracellular enzymatic redox processes, which are essential for cellular respiration, metabolism, and protein synthesis.^{7,8} Such cellular functions as energy storage and signal transduction involve electron transfer (ET) and ion transfer (IT) reactions.^{7,9} Changes in the intracellular redox state can be related to various pathological conditions, for example, oxidative stress¹⁰ and cancer.¹¹

Intracellular redox activity can be probed noninvasively by measuring the rate of transmembrane charge transfer (CT).^{12–14} Such experiments were typically performed using large cell populations and suffered from slow mass-transfer rate (minute time scale) and signal averaging. Ultramicroelectrode (UME) measurements made at the level of a single cell are much faster and provide valuable information that is hard to extract from the averaged signal produced by a large number of cells. Recently, we employed scanning electrochemical microscopy (SECM)¹⁵ for noninvasive probing of the redox activity of single mammalian cells¹⁶ and purple photosynthetic bacteria.¹⁷ This technique is known to be useful for studying biological systems.¹⁸ By scanning an ultramicroelectrode (UME) tip over the sample, one can obtain topographic images and image fluxes of oxygen at living cells.^{19,20}

In a feedback-mode SECM experiment, the tip ultramicroelectrode is placed in a solution containing the oxidized form of a redox mediator. The reduction of the mediator species at the tip surface produces steady-state current (i_T). If the tip is positioned near an immobilized living cell, the product of the tip reaction enters the cell and can be reoxidized there (Figure 1). This process produces an enhancement in the current flowing at the tip electrode (positive feedback), depending on the normalized tip/cell distance (d/a , where d is the separation distance and a is

- (1) Serber, Z.; Dotsch, V. *Biochemistry* **2001**, *40*, 14317.
- (2) Schuster, C.; Reese, I.; Urlaub, E.; Gapes, J. R.; Lendl, B. *Anal. Chem.* **2000**, *72*, 5529.
- (3) Clark, H. A.; Hoyer, M.; Philbert, M. A.; Kopelman, R. *Anal. Chem.* **1999**, *71*, 4831.
- (4) Travis, E.; Wightman, R. M. *Annual Review of Biophysics and Biomolecular Structure*; Annual Reviews: Palo Alto, CA, 1998; Vol. 27, p 77.
- (5) (a) Ewing, A. G.; Strein, T. S.; Lau, Y. Y. *Acc. Chem. Res.* **1992**, *25*, 440. (b) Lu, H.; Gratzl, M. *Anal. Chem.* **1999**, *71*, 2821.
- (6) Swanek, F. D.; Ewing, A. G. In *Handbook of Capillary Electrophoresis: Principles, Methods and Practice*, 2nd ed.; Landers, J. P., Ed.; CRC Press: Boca Raton, 1997; p 495.
- (7) Stryer, L. *Biochemistry*; W. H. Freeman and Co.: New York, 1995.
- (8) Mayfield, S. P.; Danon, A. *Science* **1994**, *266*, 1717.
- (9) (a) Staal, F. J. T.; Anderson, M. T.; Staal, G. E. J. *Proc. Natl. Acad. Sci. U.S.A.* **1994**, *91*, 3619. (b) Finkel, T. *FEBS Lett.* **2000**, *476*, 52.

- (10) (a) Soballe, B.; Poole, R. K. *Microbiology* **1999**, *145*, 1817. (b) Adler, V.; Yin, Z.; Tew, K. D.; Ronai, Z. *Oncogene* **1999**, *18*, 6104.
- (11) Greenberger, J. S.; Kagan, V. E.; Pearce, L.; Boriseniao, G.; Tyurina, Y.; Epperly, M. W. *Antioxidants and Redox Signaling* **2001**, *3*, 347.
- (12) Rabinowitz, J. D.; Vacchino, J. F.; Beeson, C.; McConnell, H. M. *J. Am. Chem. Soc.* **1998**, *120*, 2464.
- (13) Ertl, P.; Unterladstaetter, B.; Bayer, K.; Mikkelsen, S. R. *Anal. Chem.* **2000**, *72*, 4949.
- (14) Ikeda, T.; Kurosaki, T.; Takayama, K.; Kano, K.; Miki, K. *Anal. Chem.* **1996**, *68*, 192.
- (15) (a) Bard, A. J.; Fan, F.-R. F.; Pierce, D. T.; Unwin, P. R.; Wipf, D. O.; Zhou, F. *Science* **1991**, *254*, 68. (b) Bard, A. J.; Fan, F.-R. F.; Mirkin, M. V. In *Electroanalytical Chemistry*; Bard, A. J., Ed.; Marcel Dekker: New York, 1994; Vol. 18, pp 243–373. (c) Bard, A. J.; Mirkin, M. V., Eds.; *Scanning Electrochemical Microscopy*; Marcel Dekker: New York, 2001.
- (16) (a) Liu, B.; Rotenberg, S. A.; Mirkin, M. V. *Proc. Natl. Acad. Sci. U.S.A.* **2000**, *97*, 9855. (b) Liu, B.; Cheng, W.; Rotenberg, S. A.; Mirkin, M. V. *J. Electroanal. Chem.* **2001**, *500*, 590.
- (17) Cai, C.; Liu, B.; Mirkin, M. V.; Frank, H. A.; Rusling, J. F. *Anal. Chem.* **2002**, *74*, 114.
- (18) Horrocks, B. R.; Wittstock, G. In *Scanning Electrochemical Microscopy*; Bard, A. J.; Mirkin, M. V., Eds.; Marcel Dekker: New York, 2001, pp 445–519.
- (19) (a) Lee, C. M.; Kwak, J.; Bard, A. J. *Proc. Natl. Acad. Sci. U.S.A.* **1990**, *87*, 1740. (b) Tsionsky, M.; Cardon, Z. G.; Bard, A. J.; Jackson, R. B. *Plant Physiol.* **1997**, *113*, 895.
- (20) (a) Yasukawa, T.; Kaya, T.; Matsue, T. *Electroanalysis* **2000**, *12*, 653. (b) Yasukawa, T.; Kaya, T.; Matsue, T. *Anal. Chem.* **1999**, *71*, 4637.

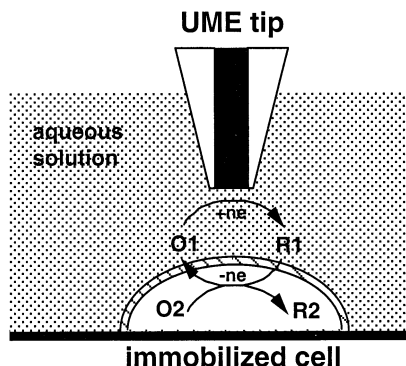
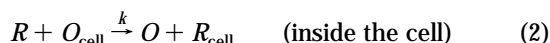
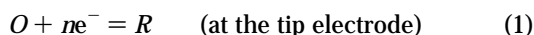


Figure 1. Schematic representation of the feedback mode SECM experiment. Oxidized form of the mediator (O1) is regenerated via a bimolecular ET reaction of R1 with cell-bound redox moieties (O2).

the tip radius). If the mediator regeneration by the cell is slow, the tip current decreases with decreasing d , because the cell surface blocks the diffusion of redox species to the tip (negative feedback). The mediated ET between the SECM tip and intracellular redox centers ($O_{\text{cell}}/R_{\text{cell}}$) can be presented as follows



(alternatively, some mediator species can be oxidized electrochemically and reduced by the cell). The tip potential is sufficiently negative so that reaction 1 is diffusion-controlled. From SECM current vs distance (i_T vs d) curves, one can extract the value of the effective heterogeneous rate constant (k) that expresses the overall rate of the mediator regeneration by the cell [reaction 2].^{16a,21}

Actually, reaction 2 is a complicated process, which includes the following steps: (i) generation of redox centers (O_{cell}) inside the cell, (ii) transport of mediator species across the cell membrane, and (iii) bimolecular ET between the mediator species and intracellular redox centers. As discussed previously,^{21,22} the overall rate (or current) of the multistep reaction under steady-state conditions can be written as a reciprocal sum of rates (or currents) of individual steps,

$$1/i_{\text{total}} = 1/i_{\text{gen}} + 1/i_{\text{membr}} + 1/i_{\text{ET}} \quad (3)$$

where i_{gen} , i_{membr} , and i_{ET} are the characteristic limiting currents for the above three stages, respectively.

$$i_{\text{gen}} = nFAk_{\text{gen}} \quad (4)$$

where n is the number of transferred electrons, F is the Faraday constant, A is the surface area and k_{gen} is the rate of generation of redox centers inside the cell per unit area. This rate is determined by cellular chemistry and was assumed to be constant during our experiment and independent of the concentration of redox mediator in solution (c°).

$$i_{\text{membr}} = nFAKD_m c^\circ / 2l \quad (5a)$$

where K is the mediator's solution-to-membrane partition coefficient, D_m is the diffusion coefficient of the mediator in the membrane (assuming $D_o = D_r$), and l is the membrane thickness. The factor 2 in the denominator reflects the fact that the mediator has to cross the cell membrane twice to produce the SECM feedback. The diffusion-limiting current through the membrane can also be expressed as²³

$$i_{\text{membr}} = nFAc^\circ P / 2 \quad (5b)$$

where $P = KD_m/l$ is the permeability coefficient.

$$i_{\text{ET}} = nFAk_{\text{ET}}c_{\text{ctr}}c^\circ \quad (6)$$

where k_{ET} ($\text{mol}^{-1}\text{cm}^4$) is the bimolecular rate constant of the ET between mediator species and intracellular redox moieties and c_{ctr} is the concentration of intracellular redox centers capable of reacting with the mediator.

Multiplying both sides of eq 3 by $nFAc^\circ$ yields

$$1/k = c^\circ/k_{\text{gen}} + 2/P + 1/k_{\text{ET}}c_{\text{ctr}} \quad (7)$$

Equation 7 will be used below to analyze concentration dependences of the effective rate constant obtained for different cells and redox mediators. Our earlier experiments showed that different human breast cell lines (i.e., nontransformed MCF-10A cells and metastatic MDA-MB-231 cells) exhibit different redox activities.^{16a} Large differences were also found between the effective rate constants of oxidation (or reduction) of different redox species by similar cells. The objectives of this work are to investigate the origins of those differences and to identify the rate-limiting steps of the overall transmembrane CT reaction under different experimental conditions. Here, our focus is on the physicochemical aspects of cellular redox reactivities. A study of biochemical mechanisms underlying the observed kinetic behavior will be reported elsewhere.²⁴

EXPERIMENTAL SECTION

Materials. $\text{Na}_4\text{Fe}(\text{CN})_6$, iodine, and KI were from Fisher Scientific (Fair Lawn, NJ). All aqueous solutions were prepared from deionized water (Milli-Q, Millipore Corp.). Menadione (General Biochemicals, Chagrin Falls, OH), 1,2-naphthoquinone (Aldrich, Milwaukee, WI), $\text{Ru}(\text{NH}_3)_6\text{Cl}_3$ (Strem Chemicals, Newburyport, MA), and other chemicals were reagent grade. Culture media, serum, and antibiotics were purchased from Invitrogen Life Technologies (Rockville, MD). All other reagents were obtained from Sigma Co. (St. Louis, MO).

Cell Culture. Mid-passage MCF-10A cells, a human breast epithelial cell line, were cultured in DMEM/F12 media (1:1) supplemented with 15% equine serum, insulin (10 $\mu\text{g}/\text{mL}$), epidermal growth factor (20 ng/mL), cholera toxin (100 ng/mL),

(21) Wei, C.; Bard, A. J.; Mirkin, M. V. *J. Phys. Chem.* **1995**, *99*, 16033.

(22) Andrieux, C. P.; Savéant, J.-M. In *Molecular Design of Surfaces*; Murray, R. W., Ed.; John Wiley & Sons: New York, 1992; p 207.

(23) Stein, W. D.; Lieb, W. R. *Transport and Diffusion across Cell Membranes*; Academic Press: Orlando, 1986; p 74.

(24) Rotenberg, S. A.; Cheng, W.; Liu, B.; Feng, W.; Michels, C. A.; Mirkin, M. V., manuscript in preparation.

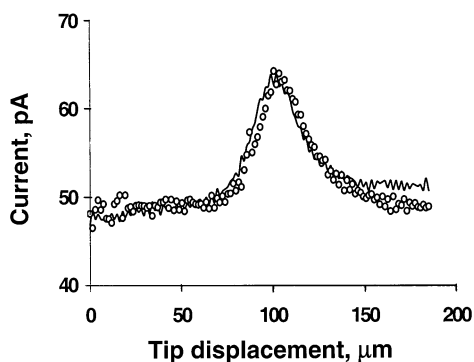


Figure 2. A 5.5- μm -radius carbon tip scanned laterally over an MCF-10A cell in phosphate buffered saline containing 30 μM 1,2-naphthoquinone. Solid line, forward scan; symbols, reverse scan. The scan rate was 20 $\mu\text{m/s}$.

and hydrocortisone (0.5 $\mu\text{g/mL}$) and maintained with penicillin (100 units/mL), streptomycin (100 $\mu\text{g/mL}$), and fungizone (0.5 $\mu\text{g/mL}$). Cells were passaged at 1:3 to 1:6 every 3–4 days. MDA-MB-231 cells were cultured in Iscove's Modified Dulbecco's Medium with L-glutamine, 10% fetal bovine serum, and 1% penicillin/streptomycin. Prior to each experiment, adherent cells that had been plated at low density in a 60-mm plastic culture dish were washed with phosphate buffered saline (153 mM Na^+ , 4 mM K^+ , 1 mM Ca^{2+} , 1 mM Mg^{2+} , 144 mM Cl^- , and 10 mM phosphate, pH 7.4).

Instrumentation and Procedures. A two-electrode setup was employed for voltammetry and SECM experiments. A 0.25-mm AgCl-coated Ag wire served as a reference electrode. Pt UME tips (5- μm radius) and carbon UME tips (5.5- μm radius) were prepared as described previously.^{15b,c}

All measurements were performed at ambient temperature in a plastic culture dish mounted on a horizontal stage of the SECM. The cells were immobilized on the bottom of the dish and were immersed in phosphate-buffered saline (PBS, pH 7.4) containing the redox mediator at the specified concentration. The SECM apparatus and procedure were described previously.¹⁶ Briefly, two types of feedback mode experiments were performed: (i) the i_T was recorded as a function of the tip position as the tip was moved laterally in a horizontal (x - y) plane a few micrometers above the cell surface, and (ii) i_T vs d curves were obtained by positioning the tip above the cell and slowly moving it vertically down to the cell surface. The data were acquired using software generously provided by D. O. Wipf (Mississippi State University). The analysis of i_T - d curves was based on an earlier model.²¹

In chronocoulometric experiments, the current vs time curves were obtained by positioning the tip in a close proximity of the cell, keeping it at rest potential for a few minutes and then instantaneously switching the tip potential to the value corresponding to diffusion-controlled reduction (or oxidation) of the redox mediator. The tip current was recorded as a function of time. The total amount of those redox centers initially present in the cell was evaluated by integrating the tip current vs time dependence, as discussed below.

SECM measurements are noninvasive in that the microprobe does not touch the cell surface, and its presence does not cause significant changes in cellular redox activity. This noninvasive property is illustrated by Figure 2, in which the tip was scanned

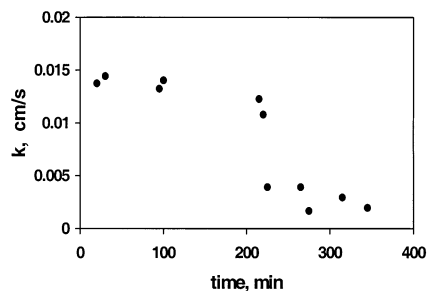


Figure 3. Changes in redox activity of MCF-10A cells with time. The tip was 5.5- μm -radius carbon fiber. The mediator was 30 μM 1,2-naphthoquinone.

twice over the same MCF-10A cell. An essentially retraceable current profile indicates that the cellular redox response was not affected by the scanning probe. Moreover, an abrupt major change in i_T is observed if the tip accidentally touches the cell surface.^{16b} Thus, one can detect and eliminate artifacts caused by the tip/cell interactions.

Because the standard potentials of quinone mediators are negative with respect to oxygen, the deaeration of solutions was necessary in experiments with those mediators. Before a set of measurements, oxygen was removed by purging a small volume (~ 5 mL) of aqueous solution covering the cells with nitrogen for 15–20 min. Between measurements, the concentration of oxygen was kept low by creating a nitrogen blanket above the solution. After finding an immobilized cell, a flow of nitrogen was quickly passed through the solution. The nearly complete removal of O_2 was evident from cyclic voltammetry. To prevent damage to the cells, oxygen was completely removed from the medium for only a brief period that immediately preceded the actual measurements, for example, ~ 3 min for obtaining an approach curve.

Cell Viability Assays. Two types of viability assays were performed to ensure that the cells remained alive and their activity did not significantly change during the SECM measurements (i.e., ~ 2 h). The effective rate constant of the mediator regeneration was measured for a number of MCF-10A cells for more than 5 h (Figure 3). As one can see in Figure 3, the k value remained essentially constant within the experimental uncertainty for ~ 3 h. This value [$k = (14 \pm 1) \cdot 10^{-3}$ cm/s] was very close to that measured previously^{16a} for MCF-10A cells. After ~ 3.5 h, the rate constant quickly decreased to ~ 0.002 cm/s. Further decrease in k was slower, and eventually all cells died and produced completely negative feedback ($k = 0$). Positive SECM feedback could be observed only when the redox reactant was continuously generated by the cell; dead cells gave only negative feedback.¹⁶ Therefore, the abrupt decrease in the cell redox response to a much lower (but nonzero) level may correspond to the mitochondrial death, after which some rudimentary activity could still be observed. Similar measurements were carried out for MDA-MB-231 cells and showed that those cells remained alive and active for at least 3 h.

Cell viability was also determined by Trypan Blue exclusion experiments. Living cells are able to pump out this blue dye, but dead cells cannot. Accordingly, in the presence of Trypan Blue, dead cells are blue and living cells appear unchanged in color under an optical microscope. To simulate the SECM conditions, the buffer solution in which the cells were immersed was

Table 1. Rates of Mediator Regeneration Reactions by MCF-10A Cells

redox species in solution (30 μ M)	$E_{1/2}$, mV vs Ag/AgCl	cell reaction	k , $10^{-3} \times \text{cm/s}$
menadione	-380	oxidation	4
1,4-naphthoquinone	-330	oxidation	11
1,2-naphthoquinone	-210	oxidation	14
2,6-dichloroindophenol	-90	oxidation	negative feedback
TMPD (first wave)	-30	reduction	≤ 0.1
TMPD (second wave)	380	reduction	8
I^-	500	reduction	diffusion-controlled

continuously deaerated with nitrogen. Trypan Blue solution (0.4%, v/v) was added to the buffer in a 1:1 ratio. In this way, the viability of the MDA-MB-231 and MCF-10A cells was found unchanged within 4 and 5 h, respectively. The cells gradually died after this time range. For MCF-10A cells, 20 and 50% of the cells died after 6.5 and 8 h, respectively. For MDA-MB-231 cells, 20 and 50% of the cells died after 5 and 7 h, respectively.

RESULTS AND DISCUSSION

Probing Mixed Intracellular Potentials. The driving force for reaction 2 is determined by the difference between the mixed intracellular potential and the formal potential of the redox mediator (the latter can be approximated by the reversible half-wave potential of quinone species, $E_{1/2}$). When the two values are similar, the intracellular redox potential becomes the rate-limiting factor. From the Marcus formula for a bimolecular rate constant,²⁵ one can obtain

$$k_{\text{ET}} = \text{const} \times \exp(-nF\Delta E^\circ/2RT) \quad (8)$$

where ΔE° is the difference between standard potentials of redox reactants. Although eq 8 is strictly applicable to a simpler situation of ET involving only two types of redox species (whereas a number of different intracellular redox moieties can participate in reaction 2), it clearly indicates that the apparent rate constant of intracellular oxidation (or reduction) reaction should increase with increasingly negative (or positive) formal potential of the redox mediator. However, no such correlation can be seen in Table 1, where the rate constants measured for three chemically similar quinone mediators of different potentials are compared. In each case, a quinone species was reduced to a diol at the tip.



The reduced form of a hydrophobic quinone mediator penetrated into the cell and was reoxidized via a bimolecular reaction with some intracellular redox moieties (Figure 1)



A significantly slower oxidation rate of more negative menadiol as compared to those of more positive 1,4-naphthoquinol, and 1,2-naphthoquinol indicates that for these quinone mediators, ET does not limit the rate of the overall regeneration process.

The cell can oxidize (or reduce) mediator species only if the mixed intracellular potential is more positive (or negative) than the formal potential of the mediator. To account for the data presented in Table 1, we assume that the intracellular potential is close to -100 mV. This value is significantly more positive than the formal potentials of menadione and naphthoquinone, hence the diol forms of these mediators are readily reduced by the cell, and ET is not the rate-determining step. In contrast, the cells could not oxidize 2,6-dichloroindophenol because its formal potential is more positive. For intracellular reduction of a mediator species, the formal potential of the $\text{TMPD}^{+/0}$ couple is close to the suggested value of the mixed intracellular potential, and consequently, ET to TMPD^+ was very slow. TMPD^{2+} , which has a more positive formal potential, was reduced significantly faster (see below).

The above estimate is not sufficiently precise to detect a difference between intracellular potentials in nontransformed and metastatic cells. A broader range of redox mediators capable of permeating cell membranes is needed to improve the evaluation of intracellular potential. The search for such mediators is underway in our laboratories.

Concentrations of Intracellular Redox Centers. We used two different approaches to evaluate the total concentration of intracellular redox moieties capable of oxidizing (or reducing) mediator species. One is based on the SECM theory developed for ET at the interface between two immiscible liquids.^{21,26} The SECM experiments with immobilized cells are conceptually similar to the studies of ET reactions at the liquid/liquid interface, in which the cell plays the role of the bottom liquid phase, and the aqueous solution above the cell is used as an upper liquid layer.^{16a} From theory developed for liquid/liquid systems,^{21,26} one can expect the measured k value to be independent of the mediator concentration (c°) provided that the intracellular concentration of redox centers (c_{ctr}) exceeds c° by a factor of ~ 15 . When c° is comparable to c_{ctr} , the effective rate constant should increase with decreasing c° value. This model is in agreement with Figure 4, from which one can see that k is essentially independent of $c_{\text{menadione}}^\circ$ when the latter is $\leq 20 \mu\text{M}$. Thus, the steady-state concentration of redox centers oxidizing menadione in MCF-10A cells is ~ 0.3 mM.

Similar curves were obtained for both MCF-10A and MDA-MB-231 cell lines using menadione, 1,2-naphthoquinone, and 1,4-naphthoquinone mediators. For all three mediators, k was independent of mediator concentration for $c^\circ \leq 20 \mu\text{M}$ (MCF-10A cells) and for $c^\circ \leq 13 \mu\text{M}$ (MDA-MB-231 cells). Hence, the

(25) Marcus, R. A. *J. Chem. Phys.* **1965**, *43*, 679.

(26) Barker, A. L.; Macpherson, J. V.; Slevin, C. J.; Unwin, P. R. *J. Phys. Chem. B* **1998**, *102*, 1586.

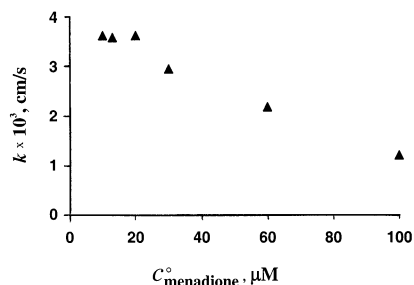


Figure 4. k vs c^o dependence for MCF-10A cells oxidizing menadiol.

concentration of intracellular centers capable of oxidizing quinone mediators is $\sim 300 \mu\text{M}$ for nontransformed breast cells and $\sim 200 \mu\text{M}$ for metastatic cells. Although the estimate may not be very accurate, the difference between the values obtained for two cell lines is reproducible. It indicates that the higher oxidative activity of MCF-10A cells can be due to the higher concentration of intracellular redox centers. On the other hand, the essentially identical c_{tr} values measured with different mediators indicate that the same intracellular moieties participate in oxidation of all three quinols. Thus, the formal potentials of those intracellular redox moieties are more positive than -210 mV , which corresponds to the formal potential of the most positive mediator species, 1,2-naphthoquinone.

The number of redox centers present in a cell and capable of reacting with a specific mediator can also be evaluated by single-cell chronocoulometry. In a chronocoulometric experiment, the concentration of redox mediator in solution is sufficiently high so that the flux of mediator species produced by the tip is significantly higher than the rate of production of redox centers in the cell. Under such conditions, the concentration of intracellular redox centers, which regenerate the mediator, should decrease with time until all of them become reduced (or oxidized). At this point, the cell is no longer capable of regenerating the mediator, and the SECM feedback becomes negative. A tip current vs time curve (Figure 5) was obtained at a $5.5\text{-}\mu\text{m}$ -radius carbon tip positioned at $\sim 5\text{-}\mu\text{m}$ distance from the surface of an MCF-10A cell in PBS containing $100 \mu\text{M}$ menadione. Immediately after the application of a negative potential to the tip, the i_T increased sharply, signifying the reduction of menadione to menadiol. A subsequent slow decrease in i_T points to the depletion of an intracellular oxidant responsible for regeneration of menadione from the diol. After $\sim 300 \text{ s}$, the tip current reached a constant value (0.19 nA), which is in agreement with SECM theory for negative feedback at the tip/substrate distance of $\sim 5 \mu\text{m}$. This indicates that the intracellular redox centers responsible for regeneration of the mediator have been completely reduced by menadiol produced at the tip. The total amount of those redox centers initially present in the cell can be evaluated by integrating the tip current vs time dependence (i.e., the shaded area above the dashed baseline in Figure 5).

To prove the complete elimination of intracellular oxidizing centers, an i_T vs d curve (curve 1 in Figure 6) was obtained immediately after a 400-s-long chronocoulometric experiment. The obtained curve fits the SECM theory for an insulating substrate (solid line). Curve 2 in Figure 6 was obtained under the same experimental conditions as curve 1, but without preceding chronocoulometry. Clearly, the tip current in curve 2 was higher, because the cell regenerated menadione.

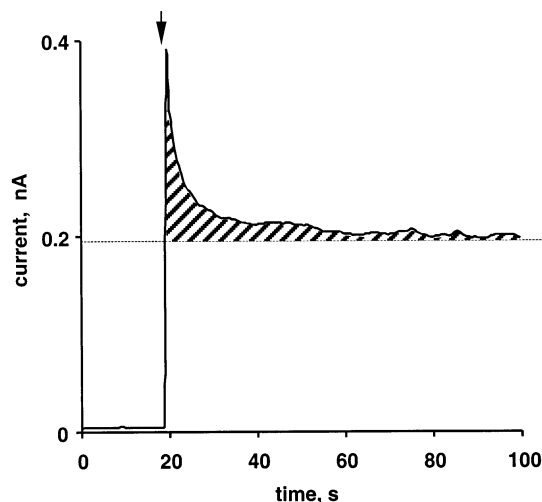


Figure 5. Current vs time dependence obtained at a $5.5\text{-}\mu\text{m}$ -radius carbon fiber UME tip positioned at a constant distance ($\sim 5 \mu\text{m}$) above an MCF-10A cell. Solution contained $100 \mu\text{M}$ menadione. Tip potential was stepped to -0.44 V vs Ag/AgCl reference. The arrow indicates when the potential was applied.

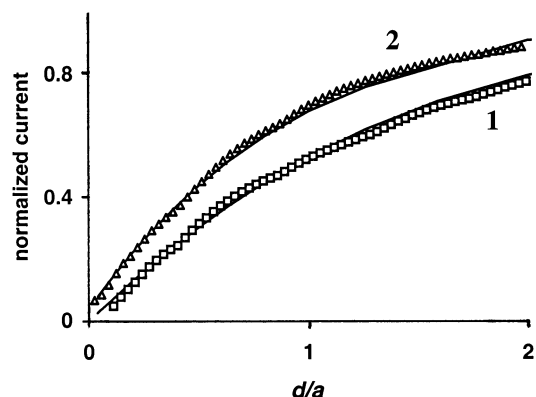


Figure 6. Current–distance curves (symbols) obtained immediately after a potentiostatic transient (curve 1) and without preceding transient (curve 2). Solid lines represent the SECM theory for an insulating substrate (curve 1)²⁷ and for finite heterogeneous kinetics (curve 2; $k = 0.0012 \text{ cm/s}$). For other parameters, see Figure 5.

By use of chronocoulometry, the numbers of intracellular redox centers capable of reacting with different mediators can be determined, as shown in Table 2. In agreement with the above analysis of i_T vs d curves, the amounts of redox moieties reacting with all quinone mediators (i.e., menadione, 1,2-naphthoquinone, 1,4-naphthoquinone) are similar for the same cell type. In contrast, a significantly (by a factor of 10) larger number of redox centers are available for reduction of I_2 , the formal potential ($+500 \text{ mV}$) of which is very positive. While the availability of an intracellular oxidant is apparently the rate-limiting factor for quinone mediators, the rapid regeneration of I^- is essentially diffusion-controlled.^{16a}

For all mediators in Table 2, the amount of the intracellular redox centers in MCF-10A cells is at least 50% higher than in MDA-MB-231 cells. The 50% difference is in agreement with the above estimates for intracellular concentrations of redox centers ($300 \mu\text{M}$ for MCF-10A cells vs $200 \mu\text{M}$ for MDA-MB-231 cells) obtained from kinetic measurements with quinone mediators. The previously observed lower redox activity of metastatic breast cancer cells^{16a} can be attributed to the lower concentration of redox

Table 2. Amounts of Intracellular Redox Centers Responsible for the Mediator Regeneration (10^{-14} mol/cell)

mediator	$E_{1/2}$, mV vs Ag/AgCl	intracellular reaction	MCF-10A	MDA-MB-231
1,2-naphthoquinone	-210	oxidation	1.05 ± 0.25	0.65 ± 0.15
1,4-naphthoquinone	-320	oxidation	1.2 ± 0.3	0.7 ± 0.2
menadione	-380	oxidation	0.9 ± 0.2	0.55 ± 0.05
KI	500	reduction	11.5 ± 0.5	6.5 ± 2.5
TMPD	380	reduction	18 ± 2	6.6 ± 1

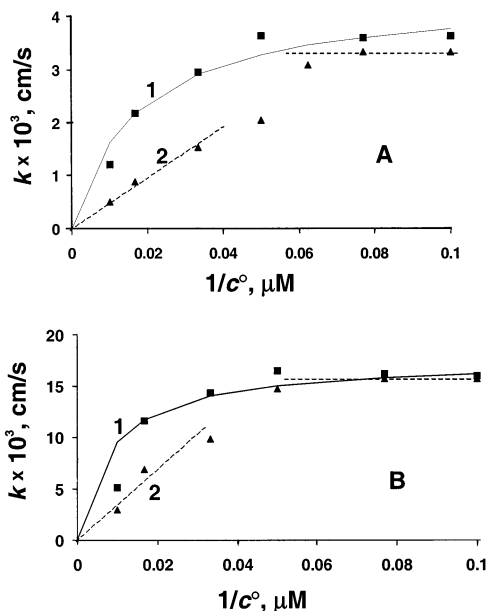


Figure 7. k vs $1/c^\circ$ dependences for regeneration of menadione (A) and 1,2-naphthoquinone (B) by MCF-10A (1) and MDA-MB-231 (2) cells. Symbols are experimental points. Solid curves (1) are calculated from eq 10. Dashed lines represent asymptotic approximations 11a and 11b. See Table 3 for the parameter values used to calculate theoretical curves.

centers. The biochemical origins of this phenomenon, which may include the overall decrease in metabolism (slower protein synthesis) in MDA-MB-231 cells and other biochemical mechanisms,^{12,28} will be addressed elsewhere.²⁴

Analysis of Concentration Dependence of the Effective Rate Constant. The dependence of the effective heterogeneous rate constant on the bulk concentration of the redox mediator (k vs $1/c^\circ$) are shown in Figure 7 for two cell lines and two different quinone mediators. These dependences can be analyzed using a simple model of mediator regeneration by the cell. As discussed above, the k values measured for menadione and naphthoquinone showed no correlation with formal potential values of those mediators. This indicates that the intracellular bimolecular ET is not the rate-limiting step of the overall reaction. Therefore, $i_{\text{ET}} \gg i_{\text{gen}}$ or i_{membr} , and eq 7 can be simplified as follows:

$$1/k \cong c^\circ/k_{\text{gen}} + 2/P \quad (10)$$

According to eq 10, the effective rate constant should be inversely proportional to the mediator concentration when the

Table 3. Membrane Permeability Coefficients and Generation Rates of Intracellular Redox Centers for MCF-10A and MDA-MB-231 Cells

mediator	k_{gen} , 10^{-9} mol $\text{cm}^{-2}\text{s}^{-1}$		P , 10^{-3} cm/s	
	MCF-10A	MDA-MB-231	MCF-10A	MDA-MB-231
menadione	0.13	0.046	7.2	6.6
1,2-naphthoquinone	0.68	0.31	32.0	31.4

overall reaction rate is limited by the generation of redox centers inside the cell, and it should be essentially independent of c° when the membrane transport is rate-limiting. This assumption is supported by the data shown in Figure 7. For both cell lines and for each redox mediator, the k vs $1/c^\circ$ plot is linear at high concentrations (when the first term in the right-hand side of eq 10 predominates, and it levels off at lower c° values (when the process rate is limited by mediator permeation). The theoretical curves calculated from eq 10 (solid curve 1 in Figure 7A,B) fit the experimental data very well, keeping in mind the approximate nature of the developed model. The parameter values can be obtained from asymptotic expressions

$$k \cong k_{\text{gen}}/c^\circ \quad \text{at high mediator concentrations} \quad (11a)$$

and

$$k \cong P/2 \quad \text{at low mediator concentrations} \quad (11b)$$

The k_{gen} and P values found from the data in Figure 7 using asymptotic expressions 11A and 11B are shown in Table 3. Comparing the P values, one can see that the rates of membrane transport of the same mediator species (i.e., either menadione or naphthoquinone) are essentially equal for MCF-10A and MDA-MB-231 cells. This finding would be expected, because the membranes of the two cell types are similar. In contrast, the k_{gen} values are significantly higher for MCF-10A cells than for MDA-MB-231 cells. This finding is consistent with the higher overall redox activity of the MCF-10A cells. The origin of the differences between k_{gen} values found for similar cells using different mediators is not clear, and there may be additional complexity not accounted for by our model.

The permeability coefficients are substantially different for menadione and 1,2-naphthoquinone. The lower P values measured for menadione may reflect the slower diffusion of this species through the membrane as a result of the difference in molecular structures (an extra methyl group in the menadione molecule). The slower membrane transport results in lower overall rates of

(27) (a) Kwak, J.; Bard, A. J. *Anal. Chem.* **1989**, *61*, 1221. (b) Mirkin, M. V.; Fan, F.-R. F.; Bard, A. J. *J. Electroanal. Chem.* **1992**, *328*, 47.

(28) Sun, X.-g.; Rotenberg, S. A. *Cell Growth Diff.* **1999**, *10*, 343.

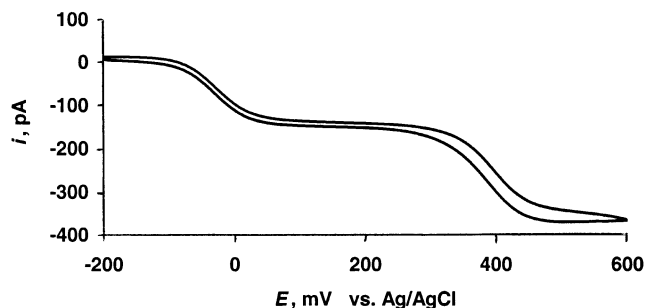


Figure 8. Steady-state voltammogram of TMPD oxidation in pH 7.4 PBS at a 11- μm -diameter carbon microdisk UME. Solution contained 100 μM TMPD. Sweep rate was 10 mV/s.

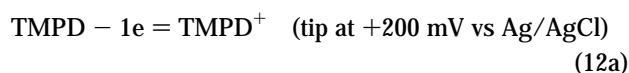
Table 4. Effect of the Mediator Concentration on the Ratio of the CT Rate Constants Measured for MCF-10A and MDA-MB-231 Cells

c° , μM	k_{10A}/k_{231}	
	1,2-naphthoquinone	menadione
10	1.0	1.1
20	1.1	1.8
30	1.5	1.9
60	1.7	2.4
100	1.7	2.4

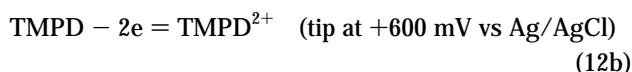
menadione regeneration by both MCF-10A and MDA-MB-231 cells (see Table 1 and ref 16a).

Significant differences in redox activities of metastatic and nontransformed breast cells were observed at relatively high quinone mediator concentrations ($c^\circ \geq 30 \mu\text{M}$).^{16a} In contrast, at lower c° ($\leq 15 \mu\text{M}$), the rate constants of oxidation of the same quinol by MCF-10A and MDA-MB-231 cells are nearly identical. The concentration dependences of the $k_{\text{MCF-10A}}/k_{\text{MDA-MB-231}}$ ratio for menadione and 1,2-naphthoquinone are presented in Table 4. Clearly, the $k_{\text{MCF-10A}}/k_{\text{MDA-MB-231}}$ ratio is somewhat higher for menadione than for 1,2-naphthoquinone, and its value increases with c° up to $\sim 60 \mu\text{M}$. These results can be used to choose optimal experimental conditions that maximize the discrimination between normal and metastatic breast cells on the basis of their redox activities.

Charged Redox Mediator: TMPD. There are several important differences between SECM experiments employing *N,N,N',N'*-tetramethyl-1,4-phenylenediamine (TMPD) and those with quinone mediators. First, TMPD is oxidized at the tip and reduced by the cell (vice versa for quinones). Second, two well-separated waves of TMPD oxidation can be observed at the tip (Figure 8). Thus, the SECM experiments can be carried out at two different tip potentials corresponding to the 1-electron



and 2-electron



oxidation.

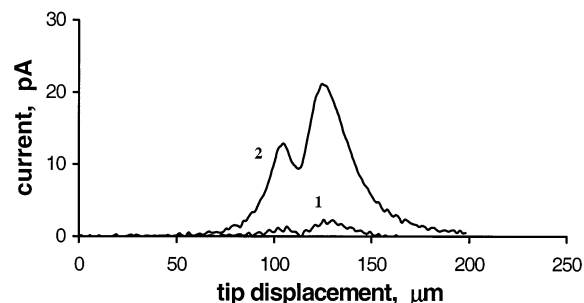
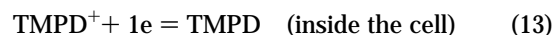
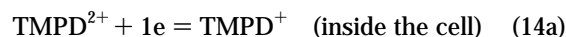


Figure 9. Current vs tip position dependencies for a 5.5- μm -radius carbon tip scanned laterally twice over the same MCF-10A cell in solution containing 30 μM TMPD. The tip potential was +200 mV (1) and +600 mV (2) vs Ag/AgCl. The scan rate was 20 $\mu\text{m/s}$.

It is noteworthy that both TMPD^+ and TMPD^{2+} species are charged. Only negative feedback responses were observed in our experiments with other charged hydrophobic mediators, such as methyl viologen ($\text{MV}^{2+/+}$) or tris(2,2'-bipyridyl)ruthenium ($\text{Ru}(\text{bpy})_3^{3+/2+}$), which can be easily transferred from water to organic solvents²⁹ and, therefore, should be capable of crossing the cell membrane. The standard potential of the $\text{MV}^{2+/+}$ couple is rather negative (-0.45 V), so MV^+ produced at the tip could be easily reoxidized inside the cell. Similarly, $\text{Ru}(\text{bpy})_3^{3+}$ is a very strong oxidizing agent, which would be rapidly reduced inside the cell. The observed negative feedback indicates that neither cationic species is taken up by the cell. Apparently, the trans-membrane IT in both cases is negligibly slow. In contrast, significant positive feedback was observed using TMPD as a mediator. Figure 9 shows two curves obtained by scanning the tip horizontally above the same MCF-10A cell in the 30 μM TMPD solution. Curve 1 was obtained at a lower tip potential (+200 mV), and curve 2 was obtained with a tip biased at +600 mV. A very small positive feedback current in curve 1 corresponds to slow reduction of TMPD^+ by the cell ($k \leq 10^{-4} \text{ cm/s}$; see Table 1).



In curve 2, the much higher i_T corresponds to a faster reduction of TMPD^{2+} inside the cell ($k = 8 \times 10^{-3} \text{ cm/s}$). The reduction of TMPD^{2+} can be either a one-electron reaction



or a two-electron process.



The two-step process (14b) is actually a combination of reactions 14a and 13. Since the latter reaction rate is much slower than the measured overall rate of TMPD^{2+} reduction by the cell, one can conclude a one-electron reaction 14a should take place inside the cell. The SECM feedback in this case is somewhat unusual; i.e., different numbers of electrons are transferred in the tip (reaction 12b) and cell (reaction 14a) processes. This was taken into account

(29) (a) Horrocks, B. R.; Mirkin, M. V. *Anal. Chem.* **1998**, *70*, 4653. (b) Nagatani, H.; Iglesias, R. A.; Fermin, D. J.; Brevet, P.-F.; Girault, H. H. *J. Phys. Chem. B* **2000**, *104*, 6869.

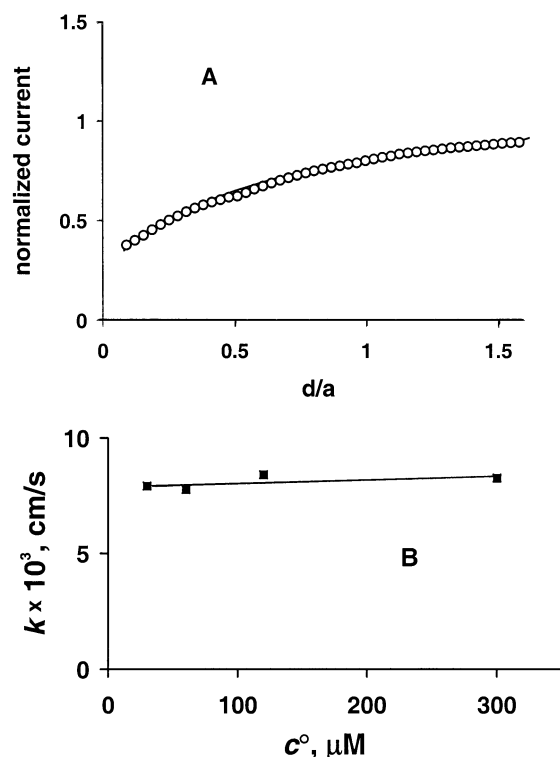
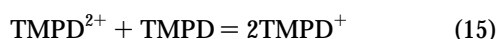


Figure 10. Experimental (symbols) and theoretical (solid line) current–distance curve for a carbon tip approaching an MCF-10A cell in PBS containing 30 μM TMPD (A) and k vs c° dependence for MCF-10A cells reducing TMPD^{2+} (B). The tip potential was +600 mV.

by using a slightly modified theoretical approximation (eq 6 from ref 21 with the feedback component of the tip current, I_s^k , divided by 2) to fit the experimental data. The experimental approach curves fit the theory very well (Figure 10A). The quality of fit was much worse when no account was given for different numbers of electrons transferred in oxidation and reduction reactions.

One can expect TMPD^{2+} species produced at the tip to participate in the comproportionation reaction in solution.



However, if this homogeneous reaction followed electrochemical oxidation of TMPD (reaction 12b), the mediator regeneration by the cell would proceed via reaction 13a. If this were the case, the same (very low) rate constant would be measured at both tip potentials, i.e., +200 and +600 mV. A much higher k value measured at more positive tip potential indicates that the species reduced by the cell is not TMPD^+ , but TMPD^{2+} . The effect of reaction 15 on the regeneration process is small because of depletion of TMPD species in the solution gap between the tip and the cell. This species is consumed at the tip (reaction 12b), and it is not regenerated by the cell, which reduces TMPD^{2+} to TMPD^+ (reaction 14a).

Unlike quinone mediators, the regeneration rates of which do not correlate with formal potential values, the higher rate of TMPD^{2+} reduction (as compared to that of TMPD^+) can be attributed to its more positive formal potential. The half-wave potential of first oxidation of TMPD (−50 mV vs Ag/AgCl; see Figure 8) is very close to the estimated value of the mixed

intracellular potential (about −100 mV). Hence, the driving force for ET is small, and the overall regeneration reaction is very slow. The half-wave potential of the second oxidation of TMPD is ~330 mV more positive, and the overall rate of the mediator regeneration is much higher.

Since the driving force is large, the ET should not be the rate-limiting step of TMPD^{2+} reduction by the cell. The rate of this process can be controlled either by membrane transport or by the availability of intracellular redox centers. The latter assumption is less plausible because of the large concentration of intracellular redox moieties capable of reducing TMPD^{2+} . The amounts of such moieties in both MCF-10A and MDA-MB-231 cells are 10–20 times larger than the corresponding values found for quinone mediators and even slightly larger than the value found for diffusion-controlled reduction of I_3^- (Table 2).

The concentration dependence of the effective rate constant (Figure 10B) is also very different from those obtained for quinone mediators (Figure 4). The k value in Figure 10B is essentially independent of c° over a broad range of mediator concentrations, from 30 to 300 μM . All of these observations are consistent with the conclusion that the TMPD regeneration rate is controlled by membrane transport. The permeability coefficient of TMPD species, $P = 16 \times 10^{-3}$ cm/s, is somewhat higher than that of menadione but lower than that of 1,2-naphthoquinone.

Unlike the transport of neutral quinone mediators, the transfer rate of ionic TMPD species across the membrane should depend on membrane potential. The latter can be changed by adding to the solution some hydrophobic ion that can permeate the cell membrane. The addition of 1 mM of tetrabutylammonium chloride (TBACl) to pH 7.4 PBS containing 30 μM TMPD resulted in a 15% decrease in the rate constant measured for MCF-10A cells. In contrast, the rate constant of 1,2-naphthoquinol oxidation by the same cell line remained practically unchanged when 100 mM TBACl was added to the solution. This difference may indicate the importance of membrane potential for multistep charge-transfer processes involving ionic species.

The above kinetic analysis has not taken into account the effect of ion transfer coupled with ET on the overall reaction rate. The uptake of TMPD^{2+} (reaction 14) results in the injection of a positive charge into the cell. To maintain electroneutrality in the cell, this charge has to be compensated by IT across the membrane (this can be, for example, the ejection of protons or other cations from the cell). The studies of ET and ion transfer coupling and its effect on the apparent cellular redox activity are underway in our laboratories.

CONCLUSIONS

The rates of oxidation–reduction reactions of various hydrophobic redox mediators by intracellular redox moieties in human breast cells have been measured by SECM at the single-cell level. A simple model was used to analyze the kinetics and identify the rate-limiting step of the multistep mediator regeneration reaction. Depending on the nature and concentration of the redox mediator, the main factor limiting the overall charge transfer rate can be either the membrane transport, the availability of intracellular redox agents, or the driving force for the ET reaction (i.e., the difference between the intracellular redox potential and the formal potential of the mediator). The k vs $1/c^\circ$ dependences obtained for different quinone mediators indicate that as the concentration

of the mediator in solution increases, the rate control shifts from membrane transport to generation of intracellular redox centers. In contrast, the transfer of a cationic redox mediator (TMPD^{2+/+}) across the membrane was always rate-limiting so that the effective rate constant exhibited no concentration dependence.

Two different methods have been developed to evaluate the intracellular concentration of redox centers capable of reacting with a specific redox mediator. The differences in redox activities of nontransformed breast cells and metastatic breast cancer cells arise from different concentrations of redox-active moieties in those cells. Biochemical processes responsible for these differences will be discussed in a future publication.²⁴ By contrast, the differences between the rate constants of regeneration of different quinone mediators by similar cells can be attributed to different membrane transport rates and redox potentials of mediator

species. The obtained kinetic data can be used to identify the experimental conditions, such as the nature and concentration of the redox mediator, that would maximize the detection of metastatic cells in a field of normal breast cells and in tissue samples.

ACKNOWLEDGMENT

The support of this work by grants from National Institutes of Health (CA91341), NSF Division of International Programs (INT0003774), and PSC-CUNY is gratefully acknowledged.

Received for review September 11, 2002. Accepted September 27, 2002.

AC020564G